Magazine of Concrete Research, 2000, **52**, No. 3, June, 169–175

Load capacity of slender reinforced concrete walls governed by flexural cracking strength of concrete

J. G. Sanjayan*

Monash University

This paper demonstrates, using experimental results and theoretical derivations, that some reinforced concrete walls may be able to carry much higher loads if the flexural cracking strength is considered in the calculation. The paper presents a theoretical derivation of a formula for estimating the axial load capacities of reinforced concrete walls subjected to eccentric axial loads as well as uniform lateral loads. A simplified, approximate version of the formula is also presented. The formula is based on the assumption that the failure of the walls is controlled by the flexural cracking strength of concrete. The paper also describes an experimental programme and reports test results for four reinforced concrete walls with varying amounts of reinforcements of varying type, namely, mesh (fabric), bar and steel fibre reinforcement. The test results show that the amount and type of reinforcement do not have any influence on the load capacity of the walls but only have an effect on the ductility of the walls. Comparisons are made with the formula and other commonly used methods of estimation. The formula estimations are much closer to the test results than the other methods for the type of walls tested.

Notation

A	bt
b	width of the wall
c	parameter defined in equation (16)
e	eccentricity of the axial load
e'	parameter defined in equation (20)
f_{cf}	flexural cracking strength of concrete
f'_c	cylinder compressive strength of concrete at 28 days
L	height of the wall
M	total bending moment
$M(x)$	bending moment at a distance x
M_{cr}	cracking moment of the wall section without any axial force
M_{max}	total bending moment at the middle of the wall
M_p	fully plastic moment
M_0	bending moment at the middle of the wall caused by lateral loads
P	axial force at failure
P_E	Euler buckling load as given in equation (9)
t	thickness of the wall
t'	parameter defined in equation (14)
x	distance measured from the top of the wall
$y(x)$	lateral deflection of the wall at distance x
Z	section modulus $= bt^2/6$
γ	parameter defined in equation (15)
Δ	deflection in the middle of the wall

* Department of Civil Engineering, Monash University, Clayton, Victoria, Australia 3168.

(MCR 755) Paper received 4 January 1999

Introduction

Reinforced concrete walls are commonly used as load-bearing structural elements. There is a new popularity in the use of reinforced concrete walls in the form of tilt-up and precast concrete walls. With these type of construction, the walls used are often very slender and made with high-strength concrete. The methods presented in the codes of practices (e.g. ACI 318[1] and AS3600[2] are inadequate for designing these walls as they are often outside the limits set by the codes. Designers therefore seek other methods to design these walls. Some of the most commonly used methods are those of SEAOSC[3], Wyatt,[4] Weiler and Nathan[5] and the Concrete Institute of Australia.[6]

0024-9831

Weiler and Nathan[5] and the Concrete Institute of Australia[6] present charts for commonly used sizes of walls. SEAOSC[3] and Wyatt[4] present simplified, approximate methods to calculate load capacities of slender reinforced concrete walls. All the methods mentioned above are based on the assumption that the failure of the wall is controlled by the yielding of the reinforcing steel.

In the SEAOSC[3] method, the load capacity is calculated when the moment at mid-height reaches the ultimate moment capacity. The deflection at mid-height is calculated on the basis of a fully cracked second moment of area and a parabolic distribution of the bending moment diagram with the ultimate moment at the middle. The applied moment at mid-height is calculated as the sum of the moments caused by lateral loads and of the moments caused by the axial loads multiplied by the eccentricity and deflection at mid-height. The axial load capacity is calculated by equating the applied moment at mid-height to the ultimate moment capacity.

The Wyatt[4] method is similar in concept except that the axial load capacity is calculated at the yield moment. The yield moment is defined as the bending moment at which the tension steel starts to yield. The curvature of the cross-section at the time when the yield moment is reached (the yield curvature) is also calculated. The deflection at mid-height is calculated assuming that the curvature distribution of the wall is sinusoidal along the height of the wall, with the yield curvature at mid-height. The axial load capacity is calculated by equating the applied moment (the sum of the moments caused by lateral loads and $P - \Delta$ effects) to the yield moment.

The other commonly used simplified methods are the fomulae presented in ACI-318[1] and AS3600.[2] Previously published research work on estimating the axial load capacity of walls includes the following: Kripanarayanan,[7] Oberlender and Everard,[8] Pillai and Parthasarathy,[9] Zielinski,[10] and Saheb and Desayi.[11] A number of formulae have been proposed by these researchers on the basis of a large number of tests on reinforced concrete walls. Most of the tests were carried out on very-small-size walls (typically 25 mm thick) and with low concrete strengths (typically 25 MPa).

The present paper sets out to demonstrate that the mode of failure controlled by the flexural cracking strength of concrete can be significant in certain types of walls. The experiments were carried out on 50 mm thick walls with concrete strengths of about 60 MPa.

Theoretical derivation

The following derivation is based on the assumption that the failure of the wall is controlled by the flexural cracking strength of the concrete. Therefore, the steel reinforcement in the concrete does not participate in the process of failure, and therefore the following derivation is equally valid for an unreinforced wall. The wall considered is subjected to an eccentric axial load P and also a uniformly distributed lateral load, as shown in Figs 1(a) and 1(b). The bending moments due to the lateral load have a parabolic distribution, as shown in Fig. 1(c).

The maximum bending moment will occur at the middle of the wall. The total bending moment at the middle of the wall, $M_{\max}$, is as given in equation (1):

$$M_{\max} = M_0 + P(\Delta + e) \tag{1}$$

The stresses across the middle section of the wall will be the sum of the stresses created by the bending moment M and the axial force P. At failure the maximum tensile stress will reach the flexural cracking strength of the concrete f_{cf} as shown in equation (2):

$$f_{\text{cf}} = \frac{M}{z} - \frac{P}{A} \tag{2}$$

where

$$z = bt^2/6 \tag{3}$$

is the section modulus,

$$A = bt \tag{4}$$

b is the width of the wall, t is the thickness of the wall and P is the axial force necessary to cause the first cracking of the concrete.

Substituting equations (1), (3) and (4) in equation (2) and rearranging,

$$\frac{bt^2}{6} f_{\text{cf}} = P(e + \Delta - t/6) + M_0 \tag{5}$$

The left-hand side of equation (5) is the cracking moment of the section, M_{cr}, in the absence of any axial force. Therefore, equation (5) becomes

$$M_{\text{cr}} = P(e + \Delta - t/6) + M_0 \tag{6}$$

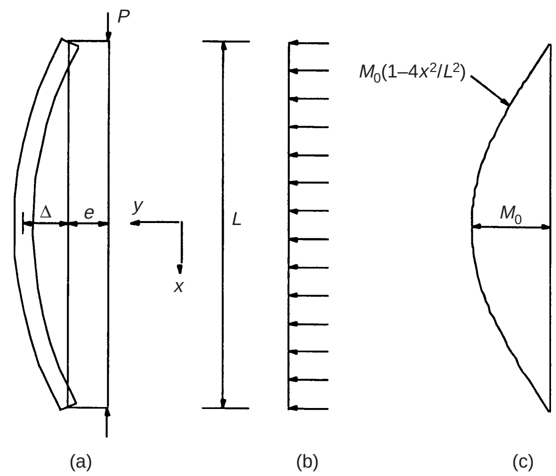

Fig. 1. Axial and lateral loads on wall: (a) eccentrically loaded wall; (b) uniform lateral load; (c) bending moment due to lateral loads

The bending moment at a distance x is as given in equation (7). Assuming a linear relationship between bending moment and curvature, the bending moment is also equal to $-EI\,\mathrm{d}^2y/\mathrm{d}x^2$, where E is the elastic modulus of the concrete and I is the second moment of area of the wall cross-section:

$$M(x) = M_0\left(1 - \frac{4x^2}{L^2}\right) + P[e + y(x)] = -EI\frac{\mathrm{d}^2y}{\mathrm{d}x^2} \quad (7)$$

Equation (7) can be solved for $y(x)$, with the boundary conditions $y(L/2) = y(-L/2) = 0$. The closed-form solution for this equation is as given in equation (8):

$$y(x) = \left(\frac{8}{\pi^2}\frac{P_E}{P}\frac{M_0}{P} + e\right)\left[\cos\left(\frac{\pi x}{L}\sqrt{\frac{P}{P_E}}\right)\sec\left(\frac{\pi}{2}\sqrt{\frac{P}{P_E}}\right) - 1\right] - \frac{M_0}{P}\left(1 - \frac{4x^2}{L^2}\right) \quad (8)$$

where

$$P_E = \frac{\pi^2 EI}{L^2} \quad (9)$$

P_E is also known as Euler buckling load.

By substituting $x = 0$ in equation (8), the deflection at the middle of the wall can be obtained:

$$\Delta = \left(\frac{8}{\pi^2}\frac{P_E}{P}\frac{M_0}{P} + e\right)\left[\sec\left(\frac{\pi}{2}\sqrt{\frac{P}{P_E}}\right) - 1\right] - \frac{M_0}{P} \quad (10)$$

The following approximation can be made to the secant function:

$$\sec\left(\frac{\pi}{2}\sqrt{\frac{P}{P_E}}\right) - 1 \approx \frac{\pi^2 P}{8(P_E - P)} \quad (11)$$

This approximation introduces less than 1% error for values of $P/P_E < 0{\cdot}35$, which is the case in the majority of slender walls found in practice. In the range $0{\cdot}35 < P/P_E < 0{\cdot}65$, the error can reach a maximum of 2%; and in the range $0{\cdot}65 < P/P_E < 0{\cdot}97$, the error can reach a maximum of 3%.

Using the approximation (equation (11)), equation (10) can be simplified as given in equation (12):

$$\Delta = \frac{\pi^2 Pe + 8M_0}{8(P_E - P)} \quad (12)$$

Substituting equation (12) in equation (6) and solving for P, we obtain equation (13):

$$P = \frac{c}{8t'}\left(\sqrt{1 + \frac{\gamma}{c^2}} - 1\right) \quad (13)$$

where

$$t' = t + \left(\frac{3\pi^2}{4} - 6\right)e \quad (14)$$

$$\gamma = 384P_E(M_{cr} - M_0)t' \quad (15)$$

$$c = 24M_{cr} + 4P_E(6e - t) \quad (16)$$

Considering the case $\gamma/c^2 \ll 1$, an approximation can be made as shown in equation (17):

$$\sqrt{1 + \frac{\gamma}{c^2}} - 1 \approx \frac{\gamma}{2c^2} \quad (17)$$

The above is a very reasonable approximation for typical walls used in practice. For example, for the range of slenderness ratio (L/t) between 20 and 40 and for M_0 varying between 0 and $0{\cdot}8M_{cr}$, the error introduced by this approximation ranges between 0·1% and 1·6%. (These error calculations are based on the assumption that the elastic modulus and flexural strength are approximately equal to $5056\sqrt{f'_c}$ and $0{\cdot}6\sqrt{f'_c}$, respectively, and the load eccentricity is equal to half the wall thickness.)

With the approximation in equation (17), equation (13) simplifies to equation (18):

$$P \approx \frac{\gamma}{16t'c} \quad (18)$$

By substituting equations (14), (15) and (16), equation (18) becomes as follows:

$$P = \frac{1}{e'}(M_{cr} - M_0) \quad (19)$$

where

$$e' = e - \frac{t}{6} + \frac{M_{cr}}{P_E} \quad (20)$$

$$M_{cr} = \frac{bt^2}{6}f_{cf} \quad (21)$$

Although equation (19) is approximate, it is a very simplified form of equation (13) and will be useful for estimating the load capacity of walls governed by the flexural cracking strength of concrete. The parameters e', M_{cr} and P_E are the effective eccentricity, cracking moment and Euler buckling load, respectively.

Experimental programme

Test specimens

The dimensions of the walls tested were as indicated in Fig. 2. Walls 1 and 2 were reinforced with a single square mesh of type F81 (8 mm nominal-diameter bars at 100 mm centre to centre) at the middle. In addition, wall 2 was reinforced with twelve reinforcing bars of 12 mm diameter. Wall 3 was reinforced with a single layer of F52 mesh (5 mm nominal diameter at 200 mm centre to centre) at the middle. Wall 4 had no conventional reinforcement but was reinforced with steel fibre reinforcements. The reinforcement details are summarized in Table 1. The reinforcement area, expressed as a percentage of the total concrete cross-sectional area, is denoted by p_x and p_y in the x and y direction, respectively.

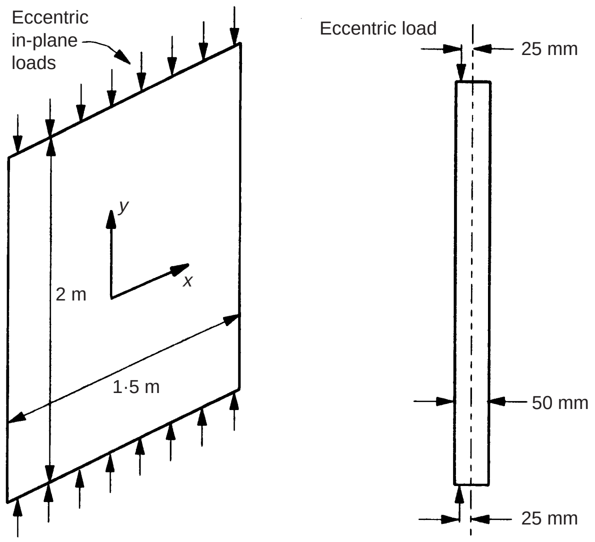

Fig. 2. Dimensions of the test walls

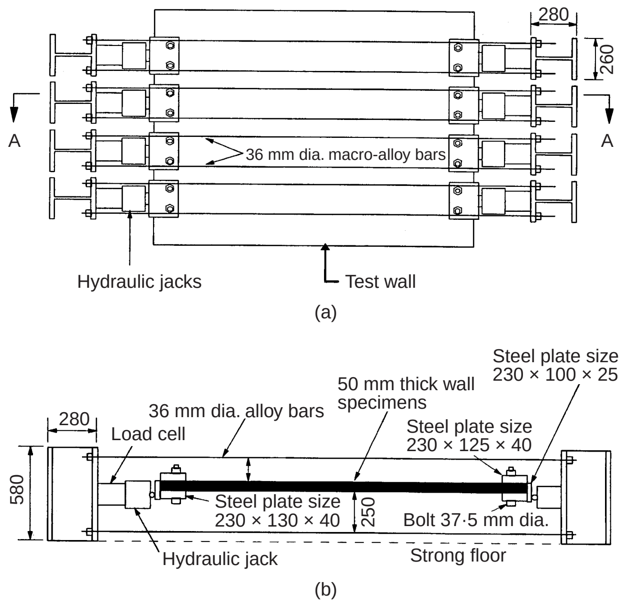

Fig. 3. Schematic diagram of test set-up (dimensions in mm): (a) plan view; (b) section A–A

The walls were cast with eight holes on each loading edge for the loading points. Additional reinforcements were provided around the holes to prevent local failure of the concrete in this region.

Concrete prisms of size 100 mm × 100 mm in cross-section and 350 mm long were prepared for testing the flexural cracking strength of the concrete. Three specimens were prepared and cured for each type of concrete. Standard cylinders (100 mm dia. and 200 mm height) were also prepared from the concrete testing the compressive strength of the concrete. All the specimens were prepared and cured according to the Australian Standard AS 1012·8.[12]

Test set-up

The specimens were tested in a horizontal position. The specimens were set up such that the self-weight was in the opposite direction to the eccentricity. Fig. 3 shows schematic drawings of the test set-up. An overview of the test frame arrangement is shown in Fig. 4. Closed loading frames were used to apply an eccentric in-plane load. Four loading frames, each having a capacity of 1000 kN, were used to apply these eccentric in-plane loads. The frames were located at equal spacings of 305 mm centre to centre. A manifold system was used to supply equal oil pressure to all the jacks so that the applied loads through all jacks were approximately equal, irrespective of their individual displacements.

Load cells were placed behind the hydraulic jacks to measure the applied loads in each frame. The eccentric load from the hydraulic jack was transferred to the steel plates by a 19 mm dia. high-strength steel rod to ensure the correct eccentricity. The steel plates were clamped to the wall by 37·5 mm dia. high-strength bolts with 500 kN pretension force in each, transferring the load to the wall by friction between the concrete and the steel plates. This arrangement was designed to avoid local failure of the concrete at the point of loading by the hydraulic jacks. A similar arrangement was used on the opposite edge, but without the hydraulic jacks.

The oil pressure applied to all the hydraulic jacks was monitored by a pressure gauge. Using the calibration data available for each hydraulic jack, the load on each jack was estimated and used as a check of the values measured by the load cells.

Lateral deflections of the wall specimens were measured using LVDTs (linear variable differential transformers) at six points along the length of the wall and three points across the length at the middle of the wall. During the tests, the walls were loaded at a slow rate (approximately 10 kN/min). At every 10 kN increment, the load was held for approximately one minute before a further increment was applied.

Table 1. Reinforcement details of the walls

Wall No.	Reinforcement arrangement	Reinforcement, y direction		Reinforcement, x direction	
		Area: mm^2	p_y: %	Area mm^2	p_x: %
1	F81 mesh	741	0·99	939	0·94
2	F81 mesh + 12 Y12 bars	2099	2·80	939	0·94
3	F52 mesh	157	0·21	177	0·18
4	Fibre steel	918	1·22	1244	1·22

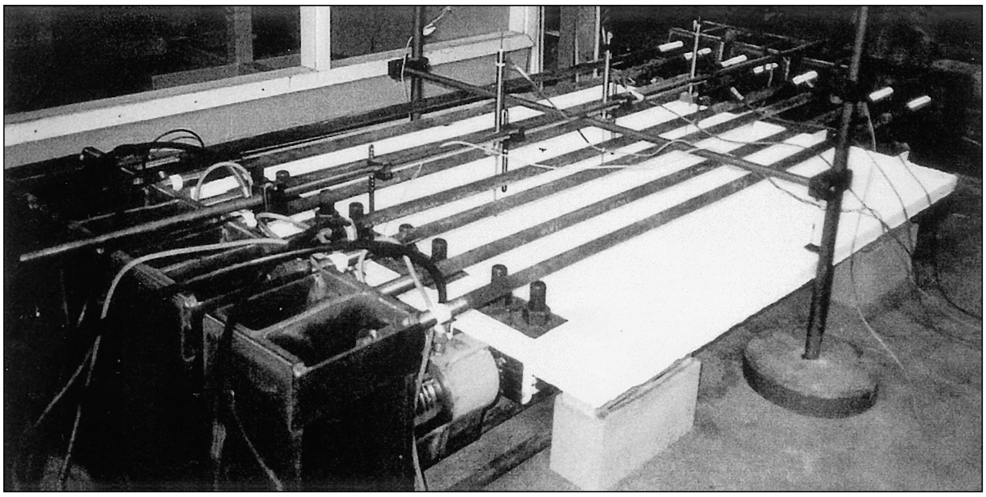

Fig. 4. Overview of test set-up

Results

The results of the tests of the material properties are presented in Table 2. The reinforcement was tested for tensile strength by testing three samples from the mesh and bars. The compressive strength of the concrete was measured by testing cylinders according to the Australian Standard AS 1012·9.[13] The flexural strengths of the concretes were obtained by testing the prisms as simple beams with third-point loading according to the Australian Standard AS 1012·11.[14]

On the basis of the results in Table 2, the first cracking moment (M_{cr}) and the fully plastic moment (M_p) were calculated; they are presented in Table 3. The values give some indication of the relative influence of the reinforcement and the flexural strength of the concrete. It should be noted that these values do not include the effects of the axial force.

Figure 5 shows a photograph of wall 1 after the test. The cracks are parallel, in the direction perpendicular to the loading direction, and are well distributed. In walls 3 and 4, the cracks were not as well distributed as in walls 1 and 2. This is due to the low levels of reinforcement present in walls 3 and 4.

In all walls except for wall 2, the peak load was reached at the same time as a flexural crack appeared. Therefore, it appears from the observations that the peak loads of walls 1, 3 and 4 were governed by the flexural cracking strength of the concrete.

The total load applied to each wall is plotted versus the deflection at the middle of the wall in Fig. 6 The deflections at the middle of the walls were measured at three points: one at the centre and two close to the edges on either side. All three deflections were found to be very close to each other.

Regardless of the varying amounts and type of reinforcement in the walls, the peak loads of the walls are more or less the same. This also indicates that the load capacity is controlled by the flexural cracking strength of the concrete rather than the amount or type of steel reinforcement. In wall 2, it seems that the load

Table 3. First cracking and fully plastic moments

Wall No.	1	2	3	4
First cracking moment M_{cr}: kN m	3·05	3·05	3·05	3·14
Fully plastic moment M_p: kN m	8·61	14·97	1·95	0

Table 2. Results for material properties

Wall No.	Age at test day: days	Strength of concrete at test day: MPa		Steel strength: MPa	
		Compressive strength	Flexural strength	Yield	Ultimate
1	28	58·5		518	648
2	31	59·0	4·88	518 (mesh) 450 (bar)	648 (mesh)
3	31	59·0		506	613
4	35	60·5	5·02		

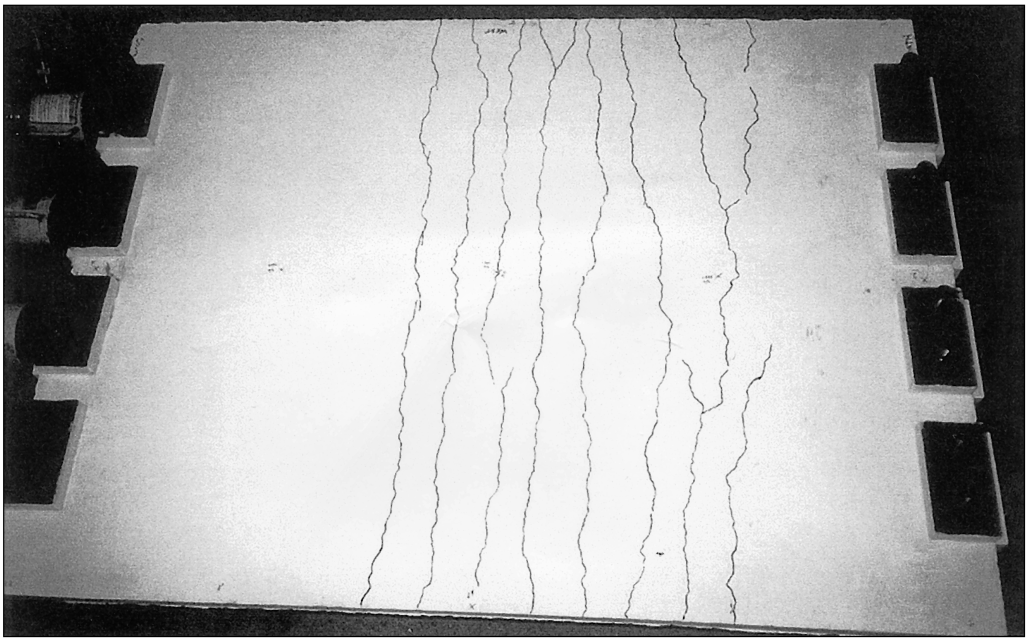

Fig. 5. Crack pattern of wall 1

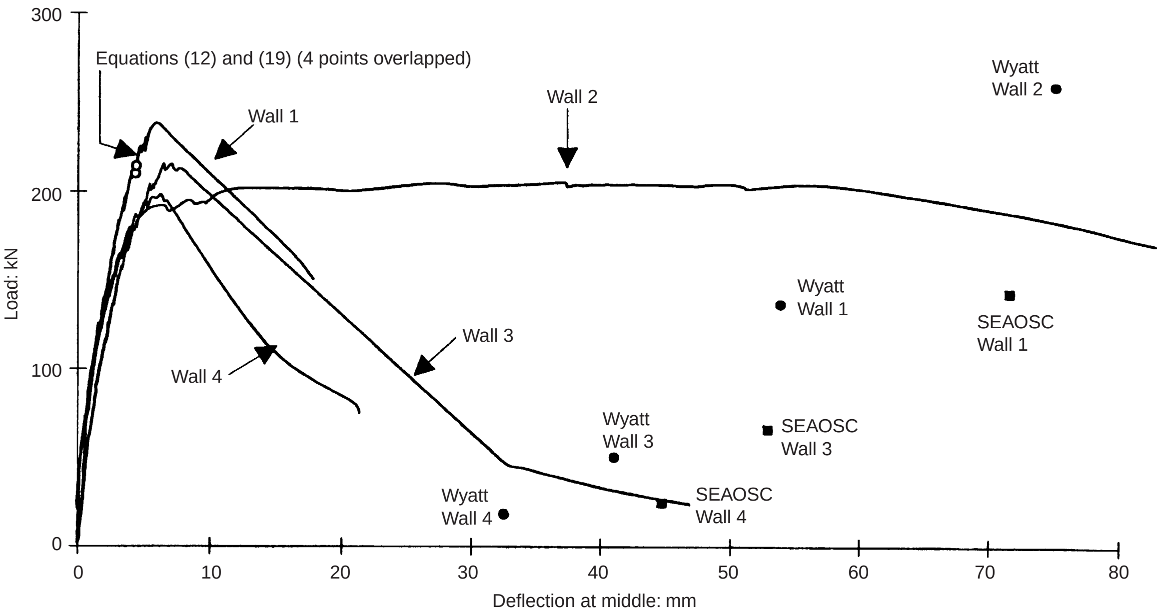

Fig. 6. Load versus deflection for the walls

capacities provided by the steel reinforcement and by the flexural cracking strength of the concrete are of similar magnitude. The post-peak behaviour of the walls, however, is significantly influenced by the amount and type of reinforcement. Wall 4, which was reinforced with fibre reinforcement but had no conventional reinforcement, exhibited the most brittle type of failure, whereas wall 2, which had the greatest amount of conventional reinforcement, exhibited a highly ductile behaviour.

Figure 6 also shows the peak load calculated on the basis of the formula proposed in this paper (equation (17)). The corresponding deflection at peak load was calculated using equation (10) for the purpose of plotting the points in Fig. 6. The peak load and deflection estimated on the basis of the formula are very close to the peak points obtained from the tests. For the purpose of these calculations, the elastic modulus was assumed to be $E = 5056\sqrt{f'_c}$. It should be noted that the self-weight of the panel was acting in the opposite direction to the eccentricity. Therefore, the moment M_0 is negative in equation (17).

Comparisons were also made with estimations of the load capacity on the basis of the methods recommended by SEAOSC[3] and Wyatt.[4] These comparisons are presented in Table 4. The estimated peak loads and deflections are also plotted in Fig. 6 as points, which are to be compared with the peak points of the experimental curves. As mentioned before, the self-weight was acting in such a direction as to increase the load capacity. This is the reason why the load capacity of wall 4 is not zero, even though the yield and ultimate moment of the wall are zero according to the Wyatt and SEAOSC methods.

The SEAOSC method assumes that all the reinforcing steel is yielding at the time the ultimate moment conditions are reached. This may not be the case in highly reinforced walls such as wall 2 (2·80% reinforcement). This partially explains the very high value estimated by the SEAOSC method for wall 2.

Conclusions

Comparisons of experimental results with theoretical estiamtions show that the formula developed in this paper gives much better estimations of load capacities than the other methods. Therefore, it is concluded that, for certain configurations of a wall (such as the ones tested), the flexural cracking strength may govern the load capacity of the wall, rather than the yielding of the steel reinforcement. This conclusion is also supported by observations made during the tests.

The amount of reinforcement of the wall does not seem to have any influence on the load capacity of the wall. However, significantly higher ductility was observed in the wall with the highest amount of reinforcement (wall 2), compared with all the other walls. It seems that the amount of reinforcement in this case was high enough to match the strength provided by the flexural cracking strength of the concrete.

The type of reinforcement (fibre steel as compared with mesh and bar reinforcements) does not seem to have any influence on the load capacity of the walls. Fibre reinforcement seems to produce a less ductile wall than the mesh and bar reinforcements.

Table 4. Comparison of estimations of load capacity

Wall No.	Experimental peak load: kN	Estimated load capacity: kN		
		Equation (19)	Wyatt[4]	SEAOSC[3]
1	238	210	137	143
2	202	210	260	1437
3	212	210	50	66
4	196	214	18	25

For walls with a typical amount of reinforcement (<1%), the commonly used design methods (SEAOSC[3] and Wyatt[4]) may be conservative for certain types of walls for estimating the load capacity, because the contribution from the flexural cracking strength is not considered.

Acknowledgements

The author gratefully acknowledges the contributions made by undergraduate student Michael Cheuk and technical staff Geoff Doddrell and Graeme Rundle.

References

1. ACI Committee 318. *Building Code Requirements for Reinforced Concrete*. American Concrete Institute, Detroit, 1993, ACI 318-93.
2. Standards Australia. *Australian Standard—Concrete Structures*. Standards Australia, Sydney, 1994, AS3600.
3. Structural Engineers Association of Southern California. *Recommended Tilt-up Wall Design*. SEAOSC, Los Angeles, 1979.
4. Wyatt J. R. Simplified design of slender tilt-up concrete walls subject to out-of-plane lateral loads. *Tilt-up Seminar*. Hobart, 1982.
5. Weiler G. and Nathan N. D. *Design of Tilt-up Concrete Wall Panels*. University of British Columbia, Vancouver, 1979.
6. Concrete Institute of Australia. *Recommended Practice for Design of Tilt-up Concrete Wall Panels*. Concrete Institute of Australia, Sydney, 1992.
7. Kripanarayanan K. M. Interesting aspects of the empirical wall design equation. *Journal of the American Concrete Institute*, 1977, **74**, No. 5, 204–207.
8. Oberlender G. D. and Everard N. J. Investigation of reinforced concrete walls. *Journal of the American Concrete Institute*, 1977, **74**, No. 6, 256–263.
9. Pillai S. U. and Parthasarathy C. V. Ultimate strength and design of concrete walls. *Building Environment* (London), 1977, **12**, 25–29.
10. Zielinski Z. A., Troitsky M. S. and Christodoulou H. Full-scale bearing strength investigation of thin wall-ribbed reinforced concrete panels. *Journal of the American Concrete Institute*, 1982, **79**, 313–321.
11. Saheb S. M and Desayi P. Ultimate strength of RC wall panels on one-way in-plane action. *Journal of the Structural Engineering Division of the ASCE*, 1989, **115**, No. 10, 2617–2630.
12. Standards Australia. As Standards Australia, *Methods of Testing Concrete—Method for Making and Curing Concrete Compression, Indirect Tensile and Flexure Test Specimens, in the Laboratory or in the Field*, 1986, Sydney, AS 1012.8.
13. Standards Australia. As Standards Australia, *Methods of Testing Concrete—Determination of the Compressive Strength of Concrete Specimens*, 1986, Sydney, 1012.9.
14. Standards Australia. As Standards Australia, *Methods of Testing Concrete—Method for the Determination of the Flexural Strength of Concrete Specimens*, 1986, Sydney, 1012.11.

Discussion contributions on this paper should reach the editor by 25 September 2000